Surface Integral Formulation for Calculating Conductor and Dielectric Losses of Various Transmission Structures

Tanmoy Roy, Tapan K. Sarkar, *Fellow, IEEE,* and Madhavan Swaminathan, *Member, IEEE*

Abstract—**The power-loss method, along with a surface integral formulation, has been used to compute the attenuation constant in microstrip and coplanar structures. This method can be used for the analysis of both open and closed structures. Using the surface equivalence principle, the waveguide walls are replaced by equivalent electric surface currents and dielectric surfaces are replaced by equivalent electric and magnetic surface currents. Enforcing the appropriate boundary condition, and E-field integral equation (EFIE) is developed for these currents. Method of moments with pulse expansion and point matching testing procedure is used to transform the integral equation into a matrix one. The relationship between the propagation constant and frequency is found from the minimum eigenvalue of the moment matrix. The eigenvector pertaining to the minimum eigenvalue gives the unknown electric and magnetic surface currents.**

I. Introduction

THE WIDESPREAD use of MIC's in recent years has caused rapid progress in its theory and technology. The very first transmission line used in MIC was, indeed, microstrip laid on the dielectric substrate, and then other transmission lines such as slot line, suspended microstrip, and so on, were introduced and improved.

Initially, the analysis for this class of transmission line was invariably a quasi-TEM approximation, except for slot line where Cohn [14] introduced a frequency-dependent solution because of its different nature. Although a quasi-TEM solution at low frequency can yield satisfactory results, at high frequency its weakness becomes apparent. To feature the frequency dependence of the lines, one must consider a hybrid mode analysis. This dispersion analysis, a hybrid mode analysis, is a generalization of the TE and TM modes studied by Swaminathan *et al.* [1]–[3]. The dominant mode in most of the waveguides and transmission lines used in microwave and MIC's are hybrid in nature. Since these modes have an electric and magnetic field in the direction of wave propagation, they cannot be fully described in terms of static capacitances and inductances. Hence, one has to introduce time varying electric and magnetic fields and solve the wave equation completely.

A method based on a surface integral formulation has been used for the computation of hybrid modes propagating in shielded microstrip lines and image lines. This formulation is based on the surface equivalence principle whereby the structure is modeled by equivalent surface currents that now represent the sources producing fields in a homogeneous medium. Hence, this work is an extension of [2].

Using the surface equivalence principle, the conducting walls and strips are replaced by equivalent electric surface currents whereas the dielectric boundaries are replaced by equivalent electric and magnetic surface currents radiating in free space. Enforcing the appropriate boundary condition an E-field integral equation (EFIE) is developed for these currents. Using method of moments [5] the integral equation is transformed into a matrix equation. The pulse basis with point matching technique is used for the transformation. Now to find the relation between frequency and propagation constant, the minimum eigenvalue of the moment matrix is plotted for whole range of values of propagation constant at particular frequency.

Once the relationship between the propagation constant and frequency is known, the fields inside the structure and on the surface of the conductors are calculated using the eigenvector pertaining to the minimum eigenvalue. The attenuation constant for various guides and structures are calculated and it has been found that our results are in good agreement with published data. This work is an extension of [3].

II. Theory

The necessary form of Maxwell's equations are given by [2]

$$\overline{E}_{zi} = \frac{1}{j\omega\epsilon_i}\overline{\nabla}_l \times \overline{H}_{li} \tag{1}$$

$$\overline{E}_{li} = -\frac{j\beta}{k_i^2 - \beta^2}\overline{z} \times \overline{\nabla}_l \times \overline{E}_{zi} - \frac{j\omega\mu_i}{k_i^2 - \beta^2}\overline{\nabla}_l \times \overline{H}_{zi}. \tag{2}$$

Equations (1) and (2) represent the relation between the electric field and magnetic field for a wave propagating along the z-direction in a medium with material properties (μ_i, ϵ_i). An $e^{-j\beta z}$ dependence has been assumed for the wave along the axial direction.

The source field relation for a dielectric loaded waveguide supporting a TM_z or a TE_z mode have already been given in [2], where subscript z denotes z-directed propagation. Since the hybrid mode is just a superposition of the TM_z and TE_z modes, the source field relation for a hybrid mode propagating in a dielectric loaded waveguide is just an extension of the derivations given in [2].

Manuscript received July 26, 1993; revised April 19, 1994. This work was supported in part by the CASE Center of Syracuse University.

T. Roy and T. K. Sarkar are with the Department of Electrical Engineering, Syracuse University, Syracuse NY 13244-1240 USA.

M. Swaminathan is with IBM, Hopewell Junction, NY 12533-0999 USA.

IEEE Log Number 9406811.

For a hybrid mode $\overline{H}_z \neq 0$ and $\overline{E}_z \neq 0$. The electric field produced by electric sources and magnetic sources supporting a hybrid mode propagating along the axial direction in a homogeneous medium with material properties (μ_i, ϵ_i) is

$$\overline{E}_{zi} = \frac{k_i^2 - \beta^2}{j\omega\epsilon_i}\overline{A}_{zi} - \overline{\nabla}_l \times \overline{F}_{li} - \frac{\beta}{\omega\epsilon_i}\overline{z}\phi_{li} \tag{3}$$

$$\begin{aligned}\overline{E}_{li} = &-\frac{\beta}{\omega\epsilon_i}\overline{\nabla}_l A_{zi} + \frac{j\beta^2}{\omega\epsilon_i(k_i^2-\beta^2)}\overline{\nabla}_l\phi_{li} \\ &- \frac{j\omega\mu_i}{k_i^2-\beta^2}[(k_i^2-\beta^2)\overline{A}_{li} + \overline{\nabla}_l\phi_{li}] \\ &+ j\beta\overline{z} \times \overline{F}_{li} - \overline{\nabla}_l \times \overline{F}_{zi}.\end{aligned} \tag{4}$$

In the above equations

$$\overline{A}_{zi} = \oint \overline{J}_z G(\sqrt{k_i^2-\beta^2}R)\, dl'$$

$$\overline{F}_{li} = \oint \overline{M}_l G(\sqrt{k_i^2-\beta^2}R)\, dl'$$

with the electric current $\overline{J}_z$ and magnetic current $\overline{M}_l z$-directed and transversely directed (represented by subscript l), respectively.

$$\overline{A}_{li} = \oint \overline{J}_l G(\sqrt{k_i^2-\beta^2}R)\, dl'$$

$$\phi_{li} = \oint \overline{\nabla}_l' \cdot \overline{J}_l G(\sqrt{k_i^2-\beta^2}R)\, dl'$$

$$\overline{F}_{zi} = \oint \overline{M}_z G(\sqrt{k_i^2-\beta^2}R)\, dl'$$

with the electric current $\overline{J}_l$ and magnetic current $\overline{M}_z$ transversely directed and z-directed, respectively. The Green's function $G(\sqrt{k_i^2-\beta^2}R)$ is given by

$$G(\sqrt{k_i^2-\beta^2}R) = \frac{1}{4j}H_0^{(2)}(\sqrt{k_i^2-\beta^2}R)$$

where $H_0^{(2)}$ is the zeroth order Hankel function of the second kind and R is the distance between the source and field co-ordinates given by $R = \sqrt{(x-x')^2+(y-y')^2}$. The primed variables represent the source and unprimed variables represent the field.

The Fig. 1 shows a dielectric loaded waveguide where C_c and C_d denote the contour of the conductor and dielectric, respectively, whereas S_c and S_d denote the surface of the conductor and dielectric, respectively. Using the equivalence principle and the continuity of tangential electric and magnetic fields on the surface S_d (Fig. 2), the electric field integral equations are

$$\left.\begin{aligned}\overline{n}_c \times \overline{E}_0(\overline{J}_c, \overline{J}_d, \overline{M}_d) = 0 \quad &\text{on } S_c^+ \\ \overline{n}_d \times \overline{E}_0(\overline{J}_c, \overline{J}_d, \overline{M}_d) = 0 \quad &\text{on } S_d^-\end{aligned}\right\} \text{in medium}(\mu_0, \epsilon_0)$$

$$\overline{n}_d \times \overline{E}_1(-\overline{J}_d, -\overline{M}_d) = 0 \quad \text{on } S_d^+ \text{in medium}(\mu_1, \epsilon_1). \tag{5}$$

In the above equations, the currents $\overline{J}_c, \overline{J}_d$ and $\overline{M}_d$ are both axially directed and transversely directed since a hybrid mode is propagating in the waveguide.

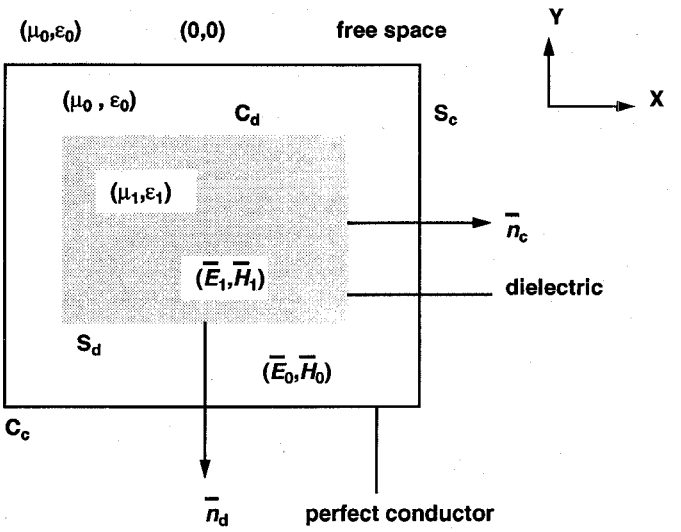

Fig. 1. Dielectric loaded waveguide.

Method of moments is used to reduce the (5) into a matrix equation. Since a hybrid mode is a coupling between the TM_z and TE_z modes, a total of $2(n+2m)$ unknowns are necessary to analyze the same waveguide supporting a hybrid mode, since both axially directed and transversely directed electric and magnetic currents support the hybrid mode. n and m denote the number of subsections on conductor and dielectric surfaces, respectively. The expansion functions are given as,

$$\begin{aligned}\overline{J}_{cz} &= \sum_{i=1}^{n} I_i\overline{J}_i \\ \overline{J}_{dz} &= \sum_{i=n+1}^{n+m} I_i\overline{J}_i \\ \overline{M}_{dl} &= \sum_{i=n+m+1}^{n+2m} I_i\overline{M}_i \\ \overline{J}_{cl} &= \sum_{i=n+2m+1}^{2n+2m} I_i\overline{J}_i \\ \overline{J}_{dl} &= \sum_{i=2n+2m+1}^{2n+3m} I_i\overline{J}_i \\ \overline{M}_{dz} &= \sum_{i=2n+3m+1}^{2(n+2m)} I_i\overline{M}_i.\end{aligned} \tag{6}$$

The weighting functions are given as

$$\overline{W}_c = \sum_{k=1}^{n}\overline{W}_k; \qquad \overline{W}_d = \sum_{k=n+1}^{n+m}\overline{W}_k. \tag{7}$$

Expanding the surface currents $\overline{J}_c, \overline{J}_d, \overline{M}_d$ in terms of expansion functions (6) and testing equations (5) with the set of weighting functions (7), the electric field integral equations reduces into the matrix form

$$[Z][I] = [0] \tag{8}$$

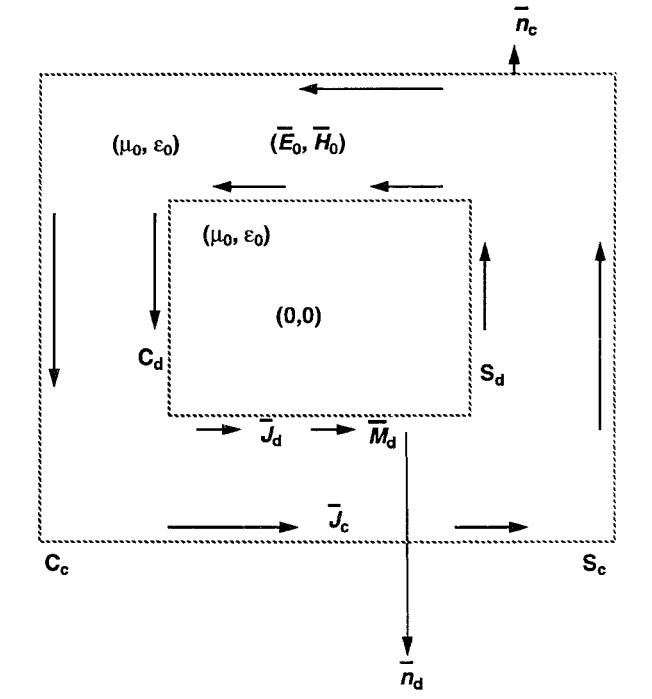

(a)

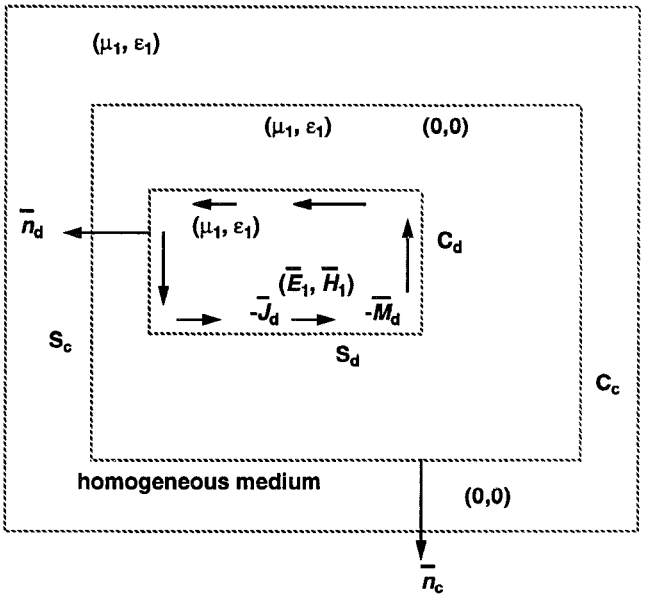

(b)

Fig. 2. (a) Equivalence for medium 0. (b) Equivalence for medium 1.

where

$$[Z] = \begin{bmatrix} Z_{TM} & 0 \\ 0 & Z_{TE} \end{bmatrix} + \begin{bmatrix} 0 & Z'_{te} \\ Z'_{tm} & Z'_{TE} \end{bmatrix}$$

and $[I]$ is a $2(n+2m)$ current vector with the first $(n+2m)$ elements representing the current coefficients necessary to produce the axial component of the electric field and the next $(n+2m)$ elements representing the current coefficients necessary to produce the transverse component of the electric field.

The sub-matrices $[Z_{TM}]$ and $[Z_{TE}]$ are $(n+2m)\times(n+2m)$ matrices with elements given in [2]. The sub-matrix $[Z'_{te}]$ ia a $(n+2m)\times(n+2m)$. The elements of this matrix

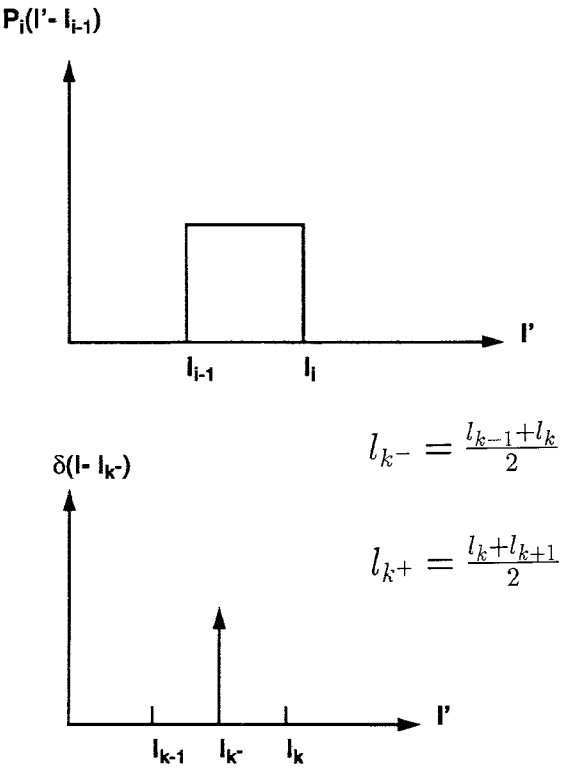

Fig. 3 Patching details.

represent the z-component of the electric field produced by the transverse electric currents $(\bar{J}_{cl})$ flowing on the walls of the conductors. Applying the equivalence principle to (4) and using the following expansion and weighting functions (Fig. 3),

$$\bar{J}_i = P_i(l' - l_{i-1})\bar{l}'_i$$

$$\text{where } P_i(l' - l_{i-1}) = \begin{cases} 1 & 0 \le l' - l_{i-1} \le l_i - l_{i-1} \\ 0 & \text{elsewhere} \end{cases} \tag{9}$$

$$\bar{W}_k = \delta(l - l_{k-})\Delta l_k \bar{l}_k$$

$$\text{where } \delta(l - l_{k-}) = \begin{cases} 1 & l = l_{k-} \\ 0 & \text{otherwise} \end{cases} \tag{10}$$

the matrix $[Z'_{te}]$ can be represented in the form

$$[Z'_{te}] = \begin{bmatrix} Z'_{11} & Z'_{12} & 0 \\ Z'_{21} & Z'_{22} & 0 \\ 0 & Z'_{32} & 0 \end{bmatrix}$$

where

$$\begin{aligned} &[Z'_{11} \quad Z'_{12} \quad 0]\,[I] \\ &= \Delta l_k \frac{\beta\sqrt{k_0^2 - \beta^2}}{4j\omega\epsilon_0} \sum_{i=1}^{n} I_i \int_{l_{i-1}}^{l_i} \left(\bar{l}'_i \cdot \frac{\bar{R}}{R}\right) \delta(l - l_{k-}) \\ &\quad \cdot P_i(l' - l_{i-1}) H_1^{(2)}(\sqrt{k_0^2 - \beta^2} R)\, dl' \\ &\quad + \Delta l_k \frac{\beta\sqrt{k_0^2 - \beta^2}}{4j\omega\epsilon_0} \sum_{i=n+1}^{n+m} I_i \int_{l_i}^{l_{i+1}} \left(\bar{l}'_i \cdot \frac{\bar{R}}{R}\right) \delta(l - l_{k-}) \\ &\quad \cdot P_i(l' - l_i) H_1^{(2)}(\sqrt{k_0^2 - \beta^2} R)\, dl' \\ &\quad k = 1, 2, \ldots, n \end{aligned}$$

$$
\begin{aligned}
&[Z'_{21} \quad Z'_{22} \quad 0]\,[I] \\
&= \Delta l_k \frac{\beta\sqrt{k_0^2-\beta^2}}{4j\omega\epsilon_0}\sum_{i=1}^{n} I_i \int_{l_{i-1}}^{l_i} \left(\bar{l}'_i \cdot \frac{\overline{R}}{R}\right)\delta(l-l_{k^+}) \\
&\quad \cdot P_i(l'-l_{i-1})H_1^{(2)}(\sqrt{k_0^2-\beta^2}R)\,dl' \\
&\quad + \Delta l_k \frac{\beta\sqrt{k_0^2-\beta^2}}{4j\omega\epsilon_0}\sum_{i=n+1}^{n+m} I_i \int_{l_i}^{l_{i+1}} \left(\bar{l}'_i \cdot \frac{\overline{R}}{R}\right)\delta(l-l_{k^+}) \\
&\quad \cdot P_i(l'-l_i)H_1^{(2)}(\sqrt{k_0^2-\beta^2}R)\,dl' \\
&\qquad k = n+1,\, n+2, \ldots, n+m
\end{aligned}
$$

$$
\begin{aligned}
&[0 \quad Z'_{32} \quad 0]\,[I] \\
&= -\Delta l_k \frac{\beta\sqrt{k_1^2-\beta^2}}{4j\omega\epsilon_1}\sum_{i=n+1}^{n+m} I_i \int_{l_i}^{l_{i+1}} \left(\bar{l}'_i \cdot \frac{\overline{R}}{R}\right)\delta(l-l_{k^+}) \\
&\quad \cdot P_i(l'-l_i)H_1^{(2)}(\sqrt{k_1^2-\beta^2}R)\,dl' \\
&\qquad k = n+1,\, n+2, \ldots, n+m.
\end{aligned}
$$

The submatrix $[Z'_{tm}]$ is also a $(n+2m)\times(n+2m)$ matrix that represents the transverse component of the electric field produced by the axial electric currents $(\overline{J}_{cz})$ flowing on the surface of the conductors and transverse magnetic currents $(\overline{M}_{cl})$ flowing on the surface of the dielectric. Applying equivalence principle to (6), the submatrix $[Z'_{tm}]$ can be represented in the form

$$
[Z'_{tm}] = \begin{bmatrix} Z''_{11} & Z''_{12} & Z''_{13} \\ Z''_{21} & Z''_{22} & Z''_{23} \\ 0 & Z''_{32} & Z''_{33} \end{bmatrix}
$$

where

$$
\begin{aligned}
&[Z''_{11} \quad Z''_{12} \quad Z''_{13}]\,[I] \\
&= \Delta l_k \frac{\beta\sqrt{k_0^2-\beta^2}}{4j\omega\epsilon_0}\sum_{i=1}^{n} I_i \int_{l_{i-1}}^{l_i} \left(\bar{l}_k \cdot \frac{\overline{R}}{R}\right)\delta(l-l_{k^-}) \\
&\quad \cdot P_i(l'-l_{i-1})H_1^{(2)}(\sqrt{k_0^2-\beta^2}R)\,dl' \\
&\quad + \Delta l_k \frac{\beta\sqrt{k_0^2-\beta^2}}{4j\omega\epsilon_0}\sum_{i=n+1}^{n+m} I_i \int_{l_i}^{l_{i+1}} \left(\bar{l}_k \cdot \frac{\overline{R}}{R}\right)\delta(l-l_{k^-}) \\
&\quad \cdot P_i(l'-l_i)H_1^{(2)}(\sqrt{k_0^2-\beta^2}R)\,dl' \\
&\quad + \Delta l_k \frac{\beta}{4}\sum_{i=n+m+1}^{n+2m} I_i \int_{l_{i-m}}^{l_{i-m+1}} (\overline{n}_k \cdot \bar{l}'_{i-m})\delta(l-l_{k^-}) \\
&\quad \cdot P_i(l'-l_{i-m})H_0^{(2)}(\sqrt{k_0^2-\beta^2}R)\,dl' \\
&\qquad k = 1,\, 2, \ldots, n
\end{aligned}
$$

$$
\begin{aligned}
&[Z''_{21} \quad Z''_{22} \quad Z''_{23}]\,[I] \\
&= \Delta l_k \frac{\beta\sqrt{k_0^2-\beta^2}}{4j\omega\epsilon_0}\sum_{i=1}^{n} I_i \int_{l_{i-1}}^{l_i} \left(\bar{l}_k \cdot \frac{\overline{R}}{R}\right)\delta(l-l_{k^+}) \\
&\quad \cdot P_i(l'-l_{i-1})H_1^{(2)}(\sqrt{k_0^2-\beta^2}R)\,dl' \\
&\quad + \Delta l_k \frac{\beta\sqrt{k_0^2-\beta^2}}{4j\omega\epsilon_0}\sum_{i=n+1}^{n+m} I_i \int_{l_i}^{l_{i+1}} \left(\bar{l}_k \cdot \frac{\overline{R}}{R}\right)\delta(l-l_{k^+}) \\
&\quad \cdot P_i(l'-l_i)H_1^{(2)}(\sqrt{k_0^2-\beta^2}R)\,dl' \\
&\quad + \Delta l_k \frac{\beta}{4}\sum_{i=n+m+1}^{n+2m} I_i \int_{l_{i-m}}^{l_{i-m+1}} (\overline{n}_k \cdot \bar{l}'_{i-m})\delta(l-l_{k^+}) \\
&\quad \cdot P_i(l'-l_{i-m})H_0^{(2)}(\sqrt{k_0^2-\beta^2}R)\,dl' \\
&\qquad k = n+1,\, n+2, \ldots, n+m
\end{aligned}
$$

$$
\begin{aligned}
&[0 \quad Z''_{32} \quad Z''_{33}]\,[I] \\
&= -\Delta l_k \frac{\beta\sqrt{k_1^2-\beta^2}}{4j\omega\epsilon_1}\sum_{i=n+1}^{n+m} I_i \int_{l_i}^{l_{i+1}} \left(\bar{l}_k \cdot \frac{\overline{R}}{R}\right)\delta(l-l_{k^+}) \\
&\quad \cdot P_i(l'-l_i)H_1^{(2)}(\sqrt{k_1^2-\beta^2}R)\,dl' \\
&\quad - \Delta l_k \frac{\beta}{4}\sum_{i=n+m+1}^{n+2m} I_i \int_{l_{i-m}}^{l_{i-m+1}} (\overline{n}_k \cdot \bar{l}'_{i-m})\delta(l-l_{k^+}) \\
&\quad \cdot P_i(l'-l_{i-m})H_0^{(2)}(\sqrt{k_1^2-\beta^2}R)\,dl' \\
&\qquad k = n+1,\, n+2, \ldots, n+m.
\end{aligned}
$$

The submatrix $[Z'_{TE}]$ is also a $(n+2m)\times(n+2m)$ matrix with elements representing the transverse component of the electric field produced by transverse electric currents $(\overline{J}_{cl})$ flowing on the conductors. This submatrix is of the form

$$
[Z'_{TE}] = \begin{bmatrix} Z'''_{11} & Z'''_{12} & 0 \\ Z'''_{21} & Z'''_{22} & 0 \\ 0 & Z'''_{32} & 0 \end{bmatrix}
$$

where

$$
\begin{aligned}
&[Z'''_{11} \quad Z'''_{11} \quad 0]\,[I] \\
&= \frac{\beta^2}{4\omega\epsilon_0(k_0^2-\beta^2)}\sum_{i=1}^{n} I_i \int_{l_{(i-1)^-}}^{l_{i^+}} (\delta(l-l_k) \\
&\quad - \delta(l-l_{k-1}))\Gamma_i(l')H_0^{(2)}(\sqrt{k_0^2-\beta^2}R)\,dl' \\
&\quad + \frac{\beta^2}{4\omega\epsilon_0(k_0^2-\beta^2)}\sum_{i=n+1}^{n+m} I_i \int_{l_{i^-}}^{l_{(i+1)^+}} (\delta(l-l_k) \\
&\quad - \delta(l-l_{k-1}))\Gamma_i(l')H_0^{(2)}(\sqrt{k_0^2-\beta^2}R)\,dl' \\
&\qquad k = 1,\, 2, \ldots, n
\end{aligned}
$$

$$
\begin{aligned}
&[Z'''_{21} \quad Z'''_{22} \quad 0]\,[I] \\
&= \frac{\beta^2}{4\omega\epsilon_0(k_0^2-\beta^2)}\sum_{i=1}^{n} \int_{l_{(i-1)^-}}^{l_{i^+}} (\delta(l-l_{k+1}) \\
&\quad - \delta(l-l_k))\Gamma_i(l')H_0^{(2)}(\sqrt{k_0^2-\beta^2}R)\,dl' \\
&\quad + \frac{\beta^2}{4\omega\epsilon_0(k_0^2-\beta^2)}\sum_{i=n+1}^{n+m} I_i \int_{l_{i^-}}^{l_{(i+1)^+}} (\delta(l-l_{k+1}) \\
&\quad - \delta(l-l_k))\Gamma_i(l')H_0^{(2)}(\sqrt{k_0^2-\beta^2}R)\,dl' \\
&\qquad k = n+1,\, n+2, \ldots, n+m
\end{aligned}
$$

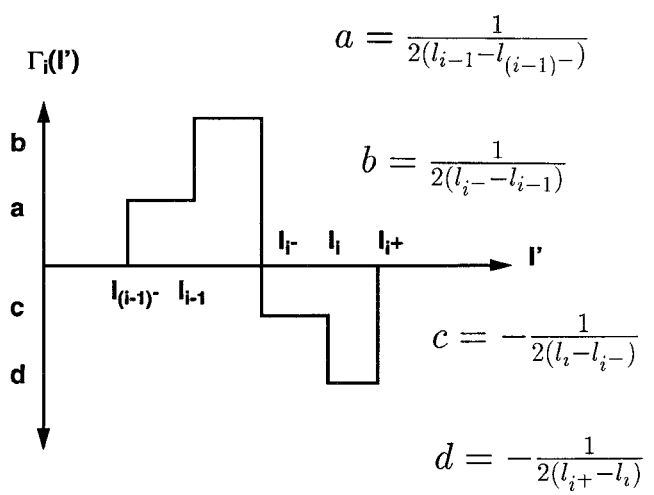

Fig. 4. Patching Function.

$$[0 \quad Z''_{32} \quad 0]\,[I] = -\frac{\beta^2}{4\omega\epsilon_1(k_1^2-\beta^2)}\sum_{i=n+1}^{n+m} I_i \int_{l_i-}^{l_{(i+1)}+} (\delta(l-l_{k+1}) - \delta(l-l_k))\Gamma_i(l')H_0^{(2)}(\sqrt{k_1^2-\beta^2}R)\,dl'$$
$$k = n+1, n+2, \ldots, n+m.$$

The $\Gamma_i(l')$'s are defined as in Fig. 4.

Based on the above equations, the electric field integral equation can be reduced to a matrix equation at a certain frequency ω and fixed propagation constant β. This matrix equation now represents a hybrid mode propagating in the guiding structure, which can be solved for the unknown expansion coefficients.

To find out the dispersion curve is to obtain a relation between propagation constant (β) and angular frequency (ω). The wavenumber k_0 appears as an argument in the matrix equation (8). For a non-trivial solution of $\overline{I}$, the moment matrix $[Z]$ has to be singular [1]. Therefore, we can say

$$\det[Z] = 0. \tag{11}$$

Equation (8) can be written as

$$[Z][I] = \lambda_{\min}[I] \tag{12}$$

where $\lambda_{\min}$ is the minimum eigenvalue of the matrix $[Z]$ and $[I]$ is the corresponding eigenvector. Assuming ω is fixed, then the propagation constant β at which $\lambda_{\min}$ is the smallest one gives the relation between β and ω. As the range of β is known ($0 \le \beta \le k_0$; $k_0 \le \beta \le \sqrt{\epsilon_r}k_0$), the relationship can be found out by a scanning procedure. The moment matrix $[Z]$ is complex, the corresponding eigenvalues are complex also. To find out the $\omega - \beta$ relation the absolute value of the eigenvalue is used in the algorithm.

III. Electromagnetic Field Distributions

The eigenvector obtained corresponding to the minimum eigenvalue ($\lambda_{\min}$) represents the equivalent current existing on the surface of the guiding structure. These equivalent current coefficients I produces exact field inside and on the surface of the guiding structure. This vector can therefore be used to calculate the fields, and hence the losses, in the structure.

The power-loss method has been used to calculate attenuation constants in the structure. The assumptions of conducting walls being perfect conductors and the dielectric medium being lossless are valid up to microwave frequencies. But in millimeter wave frequencies, the finite conductivity of the walls should be taken into account while calculating the field components. As long as the losses are small at high frequencies, the power-loss method can be used [6]. In this approach, it is assumed that the finite conductivity of the walls has only a small effect on the field configuration within the structure. The magnetic field tangential to the conducting wall of infinite conductivity is the same when the conducting wall is replaced with a conductor of finite conductivity [3]. If the structure is open, i.e., it is not surrounded by a conducting wall, the field at the surface of the dielectric bodies are not zero. Part of the guided energy lies outside of the cross-section of the dielectric body. But in the case of closed structure, the whole guided energy remains within the boundary of the conducting walls. If the external medium (e.g., air) in the case of open structure or any other medium except the dielectrics in closed structures has negligible loss, the power-loss method can be applied to calculate dielectric losses.

Using the power-loss method [6], the attenuation constant for conductor losses can be defined as

$$\alpha_c = \frac{P_L}{2P_T} \tag{13}$$

whereas the attenuation constant for dielectric losses can be defined by

$$\alpha_d = \frac{P_D}{2P_T} \tag{14}$$

where

$$P_L = \frac{1}{2}R_s\int_c |\overline{H}_{\tan}|^2\,dl \tag{15}$$

$$P_T = \frac{1}{2}\int\int_S \Re(\overline{E}\times\overline{H}^*)\cdot\overline{z}\,ds \tag{16}$$

$$P_D = \frac{1}{2}\omega\epsilon\tan\delta\int\int_{S_{diel}} |\overline{E}|^2\,ds \tag{17}$$

In the above equations, P_L is the power lost per unit length over the conducting bodies, P_T is the power transmitted, P_D is the power lost in the dielectric bodies, H_{tan} is the magnetic field tangential to the conducting surfaces for the lossless case, R_s is the surface resistance of the conducting bodies, $\Re(X)$ is the real component of X, S_{diel} is the area covered by dielectric, S is the complete cross section of the guiding structure, $\tan\delta$ is the loss tangent of the material, ϵ is the dielectric constant of the dielectric, $\overline{E}$ is the electric field inside the structure, and $\overline{H}^*$ is the complex conjugate of the magnetic field existing inside the structure. The contour C, around which the conducting loss has been calculated are the contour of all the conducting bodies present in the guiding structure. The surface resistance R_s at any frequency ω is given by

$$R_s = \sqrt{\frac{\omega\mu_0}{2\sigma}}$$

where μ_0 is the free space permeability and σ is the conductivity of the conductivity of the conducting bodies.

The term $(\overline{E}\times\overline{H}^*)\cdot z$ in (16) can be expressed in rectangular coordinate system, and after little manipulation, (16) can be written as

$$P_T = \frac{1}{2}\int\int_S \Re(E_x H_y^* - E_y H_x^*)\, ds \tag{18}$$

where x and y subscripts represent corresponding field quantities in x and y directions, respectively. From Maxwell's equations, x-directed magnetic field H_x and y-directed magnetic field H_y can be expressed as

$$H_x = -\frac{1}{j\omega\mu}\left[\frac{\partial E_z}{\partial y} + j\beta E_y\right] \tag{19}$$

$$H_y = \frac{1}{j\omega\mu}\left[\frac{\partial E_z}{\partial x} + j\beta E_x\right] \tag{20}$$

Replacing (19) and (20) in (18) and with a little algebra we get

$$P_T = \frac{1}{2}\int\int_S \Re\left[\frac{\beta}{\omega\mu}(|E_x|^2 + |E_y|^2) - \frac{1}{j\omega\mu}\left(\frac{\partial E_z^*}{\partial x}E_x + \frac{\partial E_z^*}{\partial y}E_y\right)\right] ds \tag{21}$$

The various components of the electric and magnetic fields produced by a hybrid mode propagating in the guiding structure can be calculated from the eigenvector $[I]$, corresponding to the minimum eigenvalue $\lambda_{\min}$, via (3), (4), (19), and (20). To calculate $\partial E_z/\partial x$ (20), the partial w.r.t. x has taken for (3) and expanding equivalent electric current (J_z, J_l) and magnetic current (M_l), and making some simple modification, it becomes

$$\frac{\partial E_z^*}{\partial x} = A + B + C \tag{22}$$

where

$$A = \left[\frac{\eta_i(k_i^2-\beta^2)\sqrt{k_i^2-\beta^2}}{4k_i} \cdot\sum_j I_j\int_{\Delta l_j}\frac{x-x'}{R}H_1^{(2)}p(\sqrt{k_i^2-\beta^2}R)\, dl'\right]^*$$

and

$$B = \left[-\frac{\sqrt{k_i^2-\beta^2}}{4j}\sum_j I_j\int_{\Delta l_j}\left\{-\frac{\sin\theta_j'}{R}H_1^{(2)}(\sqrt{k_i^2-\beta^2}R) - \sqrt{k_i^2-\beta^2}\frac{x-x'}{R^2}(\overline{l}_j'\times\overline{R}) \cdot H_2^{(2)}(\sqrt{k_i^2-\beta^2}R)\right\} dl'\right]^*$$

and

$$C = \left[-\frac{j\eta_i\beta}{4k_i}\sqrt{k_i^2-\beta^2} \cdot\sum_j I_j\int_{\Delta l_j}\left\{-\frac{\cos\theta_j'}{R}H_1^{(2)}(\sqrt{k_i^2-\beta^2}R) - \sqrt{k_i^2-\beta^2}\frac{x-x'}{R^2}(\overline{l}_j'\cdot\overline{R})H_2^{(2)}(\sqrt{k_i^2-\beta^2}R)\right\} dl'\right]^*$$

The subscript i denotes the ith medium, which can be either conductor or a dielectric. $\overline{l}_j'$ is the tangential unit vector on the jth subsection on the surface of conductor or dielectric, which can be expressed as

$$\overline{l}_j' = \hat{x}\cos\theta_j' + \hat{y}\sin\theta_j'.$$

$\overline{R}$ is defined as $\overline{R} = \hat{x}(x-x') + \hat{y}(y-y')$, where $\hat{x}$ and $\hat{y}$ are unit vectors along x and y directions, respectively. Here I_j is the jth component of the eigenvector $[I]$. While calculating field in the medium air (free space), our field point lies in the medium ($i = 0$), and according to equivalence principle (Fig. 2(a)), the fields in that region can be evaluated through J_{cz}, J_{dz}, M_{dl}, and J_{cl}. So, the subscript j in the summation should run through 1 to $2n + 2m$. But fields in the medium ($i = 1$) are evaluated through $-J_{cl}$ only (Fig. 2(b)). So, the j in this case should run through $n+2m$ to $2n+2m$. Δl_j is the subsection of the conducting or dielectric body along which integration of kernel is computed. Similarly $\partial E_z./\partial y$ can be expressed through J_z, J_l, and M_l and is given as

$$\frac{\partial E_z^*}{\partial y} = D + E + F \tag{23}$$

where

$$D = \left[\frac{\eta_i(k_i^2-\beta^2)\sqrt{k_i^2-\beta^2}}{4k_i} \cdot\sum_j I_j\int_{\Delta l_j}\frac{y-y'}{R}H_1^{(2)}(\sqrt{k_i^2-\beta^2}R)\, dl'\right]^*$$

and

$$E = \left[-\frac{\sqrt{k_i^2-\beta^2}}{4j}\sum_j I_j\int_{\Delta l_j}\left\{-\frac{\cos\theta_j'}{R}H_1^{(2)}(\sqrt{k_i^2-\beta^2}R) - \sqrt{k_i^2-\beta^2}\frac{y-y'}{R^2}(\overline{l}_j'\times\overline{R}) \cdot H_2^{(2)}(\sqrt{k_i^2-\beta^2}R)\right\} dl'\right]^*$$

and

$$F = \left[-\frac{j\eta_i\beta}{4k_i}\sqrt{k_i^2-\beta^2} \cdot\sum_j I_j\int_{\Delta l_j}\left\{-\frac{\sin\theta_j'}{R}H_1^{(2)}(\sqrt{k_i^2-\beta^2}R) - \sqrt{k_i^2-\beta^2}\frac{y-y'}{R^2}(\overline{l}_j'\cdot\overline{R})H_2^{(2)}(\sqrt{k_i^2-\beta^2}R)\right\} dl'\right]^*$$

$H_1^{(2)}$ and $H_2^{(2)}$ are Hankel functions of 2nd kind of order 1 and 2, respectively. $k_i = \omega\sqrt{\mu_i\epsilon_i}$ is the wave number of the medium i. $\eta_i = \sqrt{\mu_i/\epsilon_i}$ is the characteristic impedance of medium i. Equation (4) can be rewritten in more compact

form to give transverse components of electric fields as

$$\overline{E}_{li} = -\frac{\beta}{\omega\epsilon i}\overline{\nabla}_l A_{zi} + j\beta\overline{z}\times\overline{F}_{li} - j\omega\mu_i\left[\overline{A}_{li} + \frac{1}{k_i^2}\overline{\nabla}_l\phi_{li}\right] - \overline{\nabla}_l\times\overline{F}_{zi} \quad (24)$$

$$= G + H - j\omega\mu_i\left[I + \frac{1}{k_i^2}J\right] - K \quad (25)$$

where

$$G = -\frac{j\beta\eta_i}{4k_i}\sqrt{k_i^2-\beta^2}\sum_j I_j\int_{\Delta l_j}\frac{\overline{R}}{R}H_1^{(2)}(\sqrt{k_i^2-\beta^2}R)\,dl'$$

and

$$H = \frac{\beta}{4}\sum_j I_j\int_{\Delta l_j}(\overline{z}\times\overline{l}'_j)H_0^{(2)}(\sqrt{k_i^2-\beta^2}R)\,dl'$$

and

$$I = \frac{1}{4j}\sum_j I_j\int_{\Delta l_j}H_0^{(2)}(\sqrt{k_i^2-\beta^2}R)\,dl'$$

and

$$J = -\frac{\sqrt{k_i^2-\beta^2}}{4j}\sum_j I_j\int_{\Delta l_j}\Gamma_i(l')\frac{\overline{R}}{R}H_1^{(2)}(\sqrt{k_i^2-\beta^2}R)\,dl'$$

and

$$K = -\frac{\sqrt{k_i^2-\beta^2}}{4j}\sum_j I_j\int_{\Delta l_j}\frac{(\overline{z}\times\overline{R})}{R}H_1^{(2)}(\sqrt{k_i^2-\beta^2}R)\,dl'$$

In the above equations, the subscript i denotes the ith medium. If the fields to be calculated at a point lying in the medium $i = 0$ then by equivalence principle (Fig. 2(a)), the fields in that region can be evaluated through $J_{cz}, J_{cl}, J_{dz}, J_{dl}, M_{dz}$, and M_{dl}. Since G depends upon z-directed electric currents, the variable j in summation should run through 1 to $(n+m)$. H depends upon M_{dl} only. The variable j in summation runs from $(n+m+1)$ to $(n+2m)$. Since I and J both depend upon J_{cl} and J_{dl} only, the summation variable j goes from $(n+2m+1)$ to $(2n+3m)$. In the expression of K variable j in summation goes from $(2n+3m+1)$ to $2(n+2m)$, because it only depends on M_{dz}. But if the field point lies inside the medium $(i=1)$, according to equivalence principle (Fig. 2(b)), the fields can be evaluated through $-J_{dz}, -M_{dl}, -J_{dl}$, and $-M_{dz}$. In this case the summation in G goes from $n+1$ to $n+m$, in H it goes from $n+m+1$ to $n+2m$, in I and J it goes from $n+2m+1$ to $2n+3m$, whereas in K it goes from $2n+3m+1$ to $2(n+2m)$. Δl_j is the subsection of the conducting or dielectric body along which integration of kernel is computed.

The tangential component of the magnetic field on the surface of the conductor is given by the electric currents [3],

$$\overline{H}_{\tan} = -\overline{n}\times\overline{J} \quad (26)$$

where J is given by the eigenvector and $\overline{n}$ is the unit outward normal vector to the surface of the conductor.

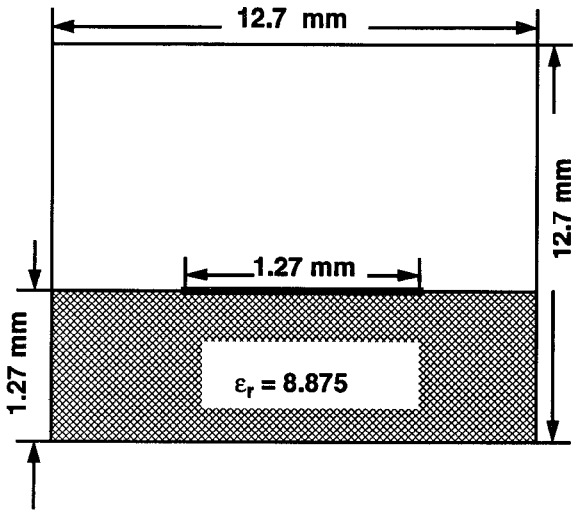

Fig. 5. Shielded microstrip line.

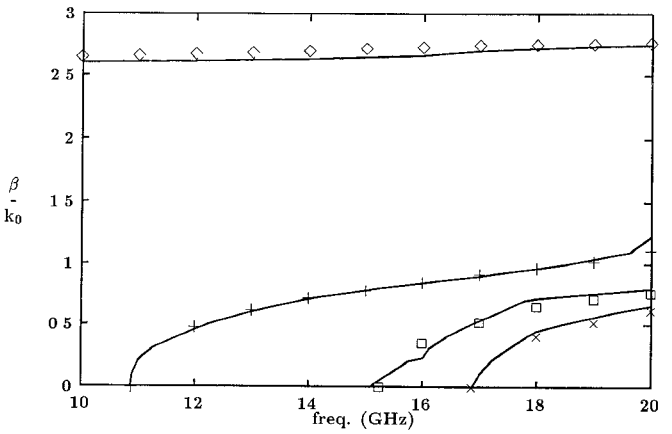

Fig. 6. Dispersion curve of shielded microstrip line.

IV. Results

A. Shielded Microstrip Line

Fig. 5 shows a shielded microstrip line that is made up of an outer conducting box, an inner dielectric body, and a conducting strip on top of the dielectric. Since the conductor fully covers the dielectric and the conducting strip, a wave propagating in this structure does not radiate any fields into the space outside the box. A relation between propagation constant β and the free space wavenumber k_0 can be found out by solving (8).

At a high frequency of operation, existence of the outer conducting body produces propagation of higher-order modes. A total of 130 subsections are used to model the structure shown in Fig. 5. Twenty four subsections are used to model the outside conducting box and five to model the inside conducting strip, whereas 36 subsections are used to model the dielectric. Altogether, 65 subsections are used for unknowns J_{cz}, J_{dz}, and M_{dl}. Another 65 subsections are used for unknowns J_{cl}, J_{dl}, and M_{dz}. The surface integral formulation is used to find the $\beta - k_0$ relation for the structure given in Fig. 5. The first four hybrid modes are given in Fig. 6. The solid lines represent the computed data using this method, whereas the points with

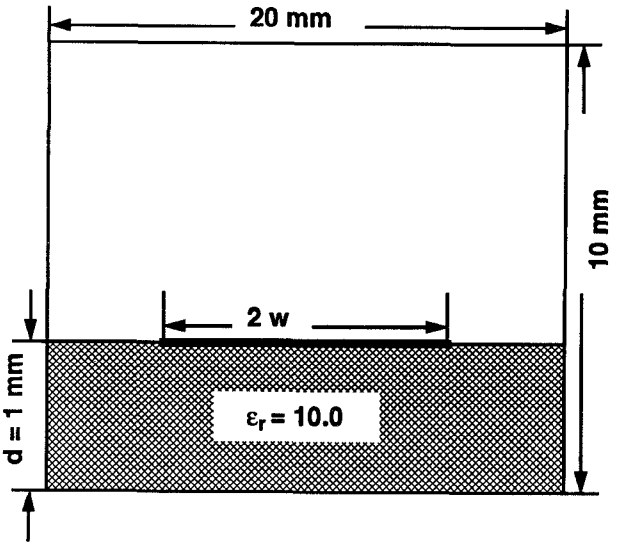

Fig. 7. Shielded microstrip line.

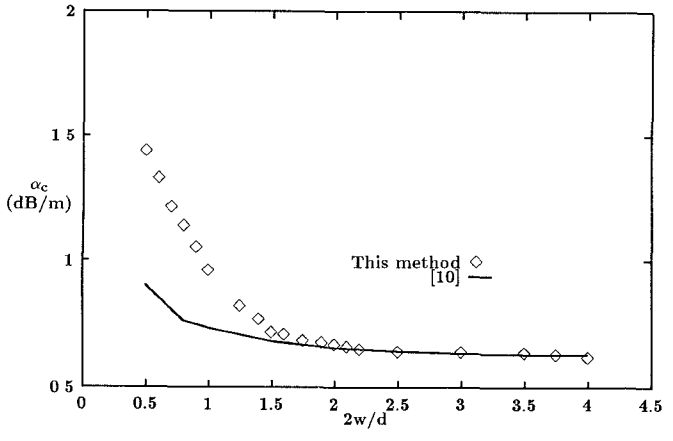

Fig. 8. Conductor losses of shielded microstrip for different linewidth.

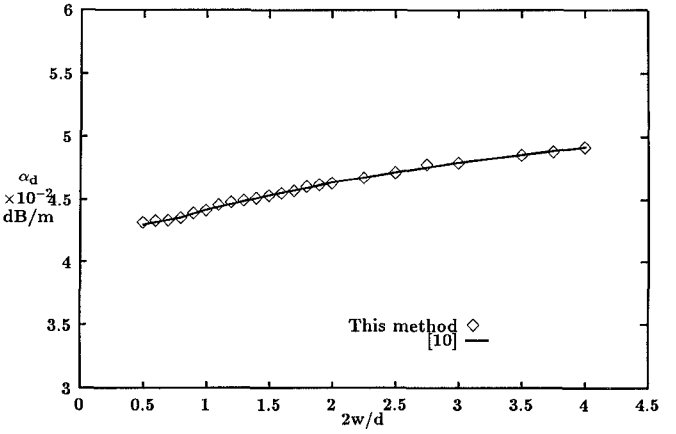

Fig. 9. Dielectric losses of shielded microstrip for different linewidth.

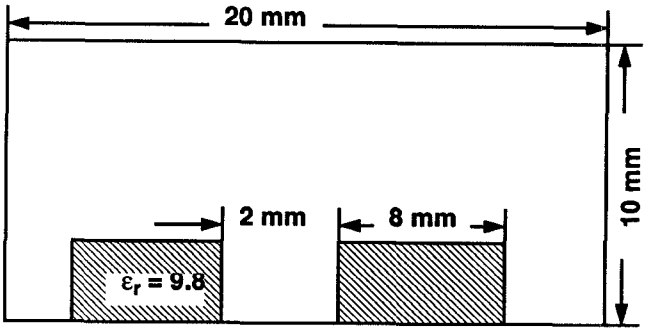

Fig. 10. Coupled image line.

boxes and pluses represent the values from [16], [10], which agree well with our computed data.

Fig. 7 shows the same shielded microstrip line with different dimensions. Conductor and dielectric losses are calculated for the structure with different $2w/h$ ratio and are shown in Fig. 8 and Fig. 9, respectively. The frequency of operation is chosen to be 1 GHz, and the $\beta - k_0$ relationship is found from the dominant mode characteristics. The conductivity of the strip and the outer conducting wall is taken to be $1/3 \times 10^8$mho-m. The solid line represents the computed data using our method, whereas the points with boxes represent the values obtained from [10]. As can be seen from Fig. 11, there is a certain discrepancy when $2w/h$ is less than 1.5. The losses in [10] are dependent on the order of solution chosen. But as the ratio $2w/h$ increases the losses are slightly dependent on the order of solution. Since the surface integral formulation does not depend upon the order of the solution, the result given by this method is more accurate.

The loss tangent $(\tan\delta)$ for the dielectric is taken to be 2×10^{-4}. The computed data agrees well with the available data [10]. In this case, the losses given in [10] do not vary with the order of solution, which can be attributed for the better agreement in this case.

B. Coupled Image Lines

Fig. 10 shows a waveguide made up of an outer conductor and two inner dielectric squares of equal dimension and same material properties separated by a distance 2 mm.

The surface integral formulation is used to obtain the propagation curve for the above mentioned structure. A total of 188 unknowns are used to obtain the $\beta - \omega$ relation, of which 94 are used for axial conductor electric surface current J_{cz}, axial dielectric electric surface current J_{dz}, and transverse dielectric magnetic surface current M_{dl}. The other 94 represent transverse electric surface current J_{cl}, transverse dielectric electric surface current J_{dl}, and axial dielectric magnetic surface current M_{dz}. The $\beta - \omega$ relation for first two hybrid modes are shown in Fig. 11. The solid lines represent the results found out by this method, whereas the points by boxes and pluses represent the results from a commercial FEM code (HFSS). Though there is good agreement for the 2nd mode, there is slight discrepancy for the first mode.

C. Image Line

Fig. 12 shows an image line that consists of a rectangular dielectric slab backed by a conducting plane. The image line analysis done in [6], assumes the conducting plane to be infinite. Though the above assumption makes the analysis

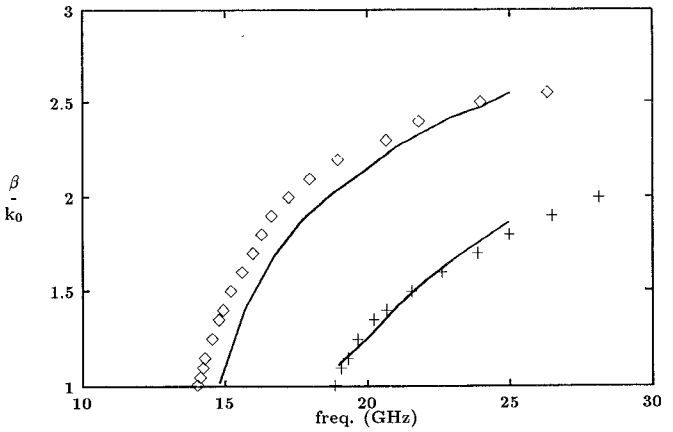

Fig. 11. Dispersion curve of coupled image lines.

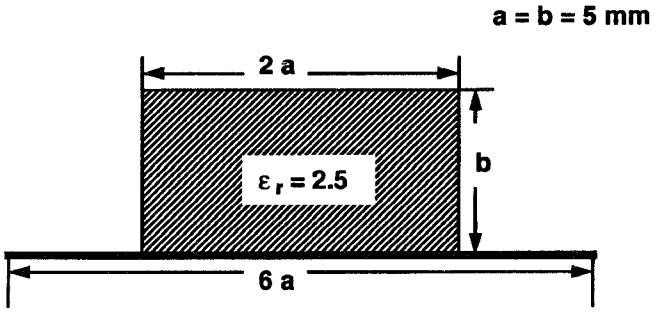

Fig. 12. Image line.

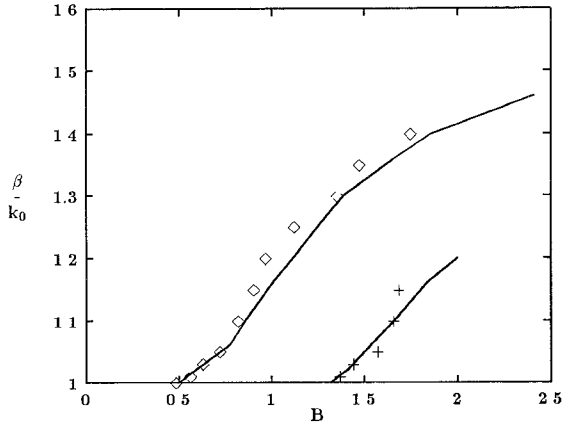

Fig. 13. Dispersion curve of an image line.

simple, the solution can not be exact when the conducting plane of finite length. In our example, the conducting plane has taken to be finite and of length $6a$, whereas the dielectric has the dimension $2a$ as one of its sides.

The surface integral formulation is used to find the dispersion curve for the image line shown in Fig. 13. A total of 120 subsections are used to model the structure. The 20 unknowns are used for each type of surface currents, which are axial conductor electric current J_{cz}, axial dielectric electric current J_{dz}, transverse dielectric magnetic current M_{dl}, transverse conductor electric current J_{cl} (in this case only J_{cx}), transverse dielectric electric current J_{dl}, and axial dielectric magnetic current M_{dz}.

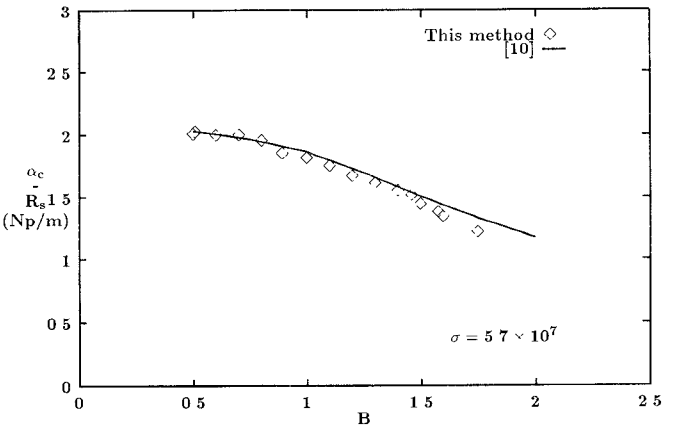

Fig. 14. Conductor loss of an image line.

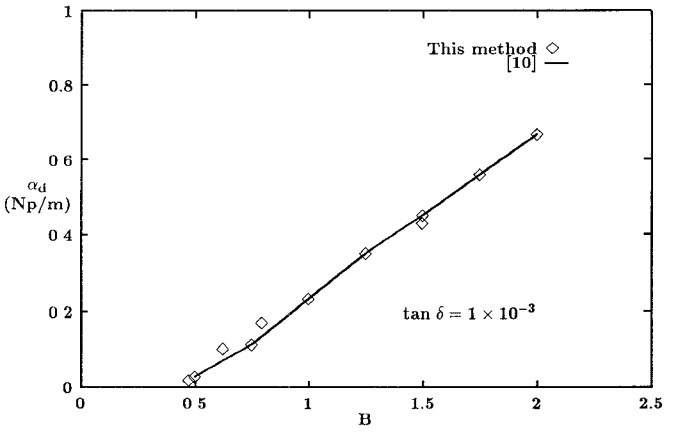

Fig. 15. Dielectric loss of an image line.

The dispersion curve for the image line for first two hybrid modes, giving the ratio of propagation constant β to the free space wavenumber k_0 as a function of normalized guide dimension B is shown in Fig. 14. The normalized guide dimension B is given by

$$B = \frac{4b}{\lambda_0}\sqrt{\epsilon_r - 1}.$$

The solid lines represents the results computed by this method whereas the boxes and pluses represent the result from [6]. The agreement of our result with [6] is good.

The attenuation constants, both for conductor and dielectric are plotted in Fig. 15, respectively. The attenuation constants has been calculated for the first mode only. The attenuation constant for the conductor is given by α_c/R_s to normalized guide dimension B. The solid line is the result computed by this method, whereas the points by boxes represent the results from [6]. The results agree well with the results given by [6].

The loss tangent for the dielectric $\tan\delta$ is assumed to be 0.001, which satisfy our criteria of low lossy material so that power-loss method can be used to calculate α_d. Fig. 16 shows attenuation constant for dielectric α_c to normalized guide dimension B. The results compared with [6] gives good agreement.

V. Summary and Conclusion

The power-loss method, coupled with the surface integral formulation, has been used to compute attenuation constant for both conductor and dielectric losses for hybrid modes in open and closed structures. A simple point matching testing procedure with pulse expansion functions has been chosen to transform the integral equation into a matrix one. After getting the relation between the propagation constant and frequency, the fields inside or on the surface of the conductors are calculated. Using the field quantities, the losses have been found out. The losses calculated are valid for hybrid modes. The computed results show good agreement with available results.

The surface integral method did not produce any spurious modes for the region $0 \leq \beta \leq k_0$. But the presence of spurious modes is observed in the region $k_0 \leq \beta \leq k_0\sqrt{\epsilon_r}$. These spurious modes can be identified looking at the eigenvector corresponding to the minimum eigenvalue. A mode can be identified as spurious using two criteria described in [2]. It is also noticed that the occurrence of spurious modes is prominent when the dielectric used in the analysis is thin (example A).

The surface integral method along with power-loss method is a very useful technique that can be used for treating complex structures to compute conducting and dielectric losses.

References

[1] M. Swaminathan, E. Arvas, T. K. Sarkar, and A. R. Djordjevic, "Computation of cutoff wavenumbers of TE and TM modes in waveguides of arbitrary cross sections using a surface integral formulation," *IEEE Trans. Microwave Theory Tech.*, vol. 38, no. 2, pp. 154–159, Feb. 1990.

[2] M. Swaminathan, T. K. Sarkar, and A. T. Adams, "Computation of TM and TE modes in waveguides based on a surface integral formulation," *IEEE Trans. Microwave Theory Tech.*, vol. 40, no. 2, pp. 285–297, Feb. 1992.

[3] M. Swaminathan, T. K. Sarkar, P. Petre, and T. Roy, "Conductor loss in hollow waveguides using surface integral formulation," *IEEE Trans. Microwave Theory Tech.*, vol. 40, no. 11, pp. 2034–2041, Nov. 1992.

[4] R. F. Harrington, *Time-Harmonic Electromagnetic Fields.* New York: McGraw-Hill, 1961.

[5] R. F. Harrington, *Field Computation by Moment Methods.* New York: MacMillian, 1968.

[6] P. Bhartia and I. J. Bahl, *Millimeter Wave Engineering and Application.* New York: Wiley, 1989.

[7] M. Abramowitz and I. Stegun, *Handbook of Mathematical Functions.* New York: Dover, 1965.

[8] F. Oberhettinger, *Fourier Transforms of Distributions and Their Inverse.* New York: Academic, 1973.

[9] M. Swaminathan, "Analysis of waveguides based on a surface integral formulation," Ph.D dissertation, Syracuse Univ., Dec. 1990.

[10] D. Mirshekar-Syahkal and J. B. Davis, "Accurate solution of microstrip and coplanar structures for dispersion and for dielectric and conductor losses," *IEEE Trans. Microwave Theory Tech.*, vol. 27, no. 7, pp. 694–699, July 1979.

[11] R. Mittra and T. Itoh, "A new technique for analysis of dispersion characteristics of microstrip lines," *IEEE Trans. Microwave Theory Tech.*, vol. 19, no. 1, pp. 47–56, Jan. 1971.

[12] R. A. Pucel, D. J. Masse, and C. P. Hartwig, "Losses in microstrip," *IEEE Trans. Microwave Theory Tech.*, vol. 16, no. 6, pp. 342–350, June 1968.

[13] B. E. Spielman, "Dissipation loss effects in isolated and coupled transmission lines," *IEEE Trans. Microwave Theory Tech.*, vol. 25, no. 8, pp. 648–656, Aug. 1977.

[14] S. B. Cohn, "Slot line on a dielectric substrate," *IEEE Trans. Microwave Theory Tech.*, vol. 17, no. 10, pp. 768–778, Oct. 1969.

[15] U. Crombach, "Analysis of single and coupled rectangular dielectric waveguides," *IEEE Trans. Microwave Theory Tech.*, vol. 29, no. 9, pp. 870–874, Sept. 1981.

[16] E. Yamashita and K. Atsuki, "Analysis of microstrip-like transmission lines by non-uniform discretization of integral equations," *IEEE Trans. Microwave Theory Tech.*, vol. 24, no. 4, pp. 195–200, Apr. 1976.

Tanmoy Roy was born in Calcutta, India, on November 30, 1967. He received the B.Tech. degree from the Indian Institute of Technology, Kharagpur, India, in 1990. He is currently enrolled in the Ph.D. program at Syracuse University.

From 1990 to 1991 he served as a software consultant in Tata Consultancy Services, India. His current research interests deal with the numerical analysis of waveguides and transmission lines.

Tapan K. Sarkar (S'69-M'76-SM'81-F'91) was born in Calcutta, India, on August 2, 1948. He received the B.Tech. degree from the Indian Institute of Technology, Kharagpur, India, in 1969, the M.Sc.E. degree from the University of New Brunswick, Fredericton, Canada, in 1971, and the M.S. and Ph.D. degrees from Syracuse University, Syracuse, NY, in 1975.

From 1975 to 1976 he was with the TACO Division of the General Instruments Corporation. He was with the General Instruments Corporation. He was with the Rochester Institute of Technology, Rochester, NY, from 1976 to 1985. He was a Research Fellow at the Gordon McKay Laboratory, Harvard University, Cambridge, MA, from 1977 to 1978. He is now a professor in the Department of Electrical and Computer Engineering, Syracuse University, Syracuse, NY. His current research interests deal with numerical solutions of operator equations arising in electromagnetics and signal processing with application to system design. He obtained one of the "best solution" awards in May 1977 at the Rome Air Development Center (RADC) Spectral Estimation Workshop. He has authored or coauthored more than 154 journal articles and conference papers and has written chapters in eight books.

Dr. Sarkar is a registered professional engineer in the state of New York.

Madhavan Swaminathan (M'91) was born on August 9, 1962 in Madras, India. He received the B.E. degree in electronics and communication from Regional Engineering College, Tiruchi, India, in 1985, and the M.S. and Ph.D. degrees in electrical engineering from Syracuse University in 1989 and 1991, respectively.

He was a graduate assistant in the Department of Electrical and Computer Engineering at Syracuse University from 1986–1990. During this period he was made a Fellow of the Northeast Parallel Archtectures Center for a period of one year. As a Fellow, he developed algorithms for the solution of large electromagnetic field problems on parallel computers. In 1990 he joined the International Business Machines Corporation, East Fishkill, NY, where he is presently working on the analysis of transmission lines for high speed integrated circuits. His research interests are in the areas of microwave transmission lines, cavity resonators and electromagnetic radiation.